Elementary Flux Modes as CRN Gears for Free Energy Transduction

Massimo Bilancioni* and Massimiliano Esposito†
Department of Physics and Materials Science, University of Luxembourg, avenue de la Faïencerie, Luxembourg City, 1511 G.D. Luxembourg
(Dated: June 3, 2024)

We demonstrate that, for a chemical reaction network (CRN) engaged in energy transduction, its optimal operation from a thermodynamic efficiency standpoint is contingent upon its working conditions. Analogously to the bicycle gear system, CRNs have at their disposal several transducing mechanisms characterized by different yields. We highlight the critical role of the CRN's elementary flux modes in determining this "gearing" and their impact on maximizing energy transduction efficiency. Furthermore, we introduce an enzymatically regulated CRN, engineered to autonomously adjust its "gear", thereby optimizing its efficiency under different external conditions.

Introduction - Free energy transduction in chemical reaction networks (CRNs) is a common phenomenon, especially in biology, where it is carried out continuously by metabolic networks to sustain life: catabolic processes degrade energetic food molecules to synthesize ATP, which is then used by anabolic processes to perform energy-demanding cellular tasks [1–4]. At the fundamental level, transduction works by coupling nonequilibrium processes. This coupling is provided by the underlying CRN and can be tight or loose, depending on whether the input and output processes are forced to occur in a fixed ratio, as in a unicyclic CRN, or not [5]. Tightly coupled CRNs are the only ones that can reach Carnot transduction efficiency [6], and for linear loosely coupled CRNs, futile cycles always reduce the transduction efficiency [7]. These clues naturally prompt the question of whether a loosely coupled CRN is always less efficient than its tightly coupled counterpart. However, this question, which originally motivated our work, is not well defined. Indeed, a loosely coupled CRN possesses not one but several possible tightly coupled (unicyclic) subnetworks to which it can be compared. These subnetworks are equivalent to elementary flux modes (EFMs) [8], widely used for metabolic pathway analysis [9, 10], which constitute the right tool for analyzing free energy transduction. Indeed, each of them can be seen as a transduction gear of the CRN, in analogy to the gears of a bicycle. In this letter, we identify the optimal EFM (gear), which depends on the operational conditions and upper bounds the CRN efficiency, Eq. (10). This result offers a way to benchmark the efficiency-optimality of metabolic networks. Its proof is based on a novel decomposition of the entropy production (EP) in terms of EFMs, Eq. (2). Metabolic gear shifting, also known as metabolic switching, is a widely observed phenomenon [11–17]. To understand how CRNs can autonomously change gear, we end our letter by presenting a simple biologically inspired CRN that optimizes its efficiency under varying external conditions by autonomously adjusting its "gears" through enzyme regulation, Fig. 3.

Elementary flux modes (EFMs) - We consider a CRN with a set of internal species X, a set of external species Y, and a set of reactions ρ. In the following, we use the CRN in Fig. 1 a) as an illustrative example. There, the external species are $Y = A_-, A_+, B_-$, and B_+. A vector $\boldsymbol{\psi}$ (in the space of reactions) is a *flux mode* if it is a cycle for the internal species: $\mathbb{S}^X \boldsymbol{\psi} = 0$, where $\mathbb{S}^X$ is the stoichiometric matrix reduced to the X species. In addition, a flux mode $\boldsymbol{\psi}_e$ is *elementary* if the set of reactions it involves, defined by its support $\mathrm{supp}(\boldsymbol{\psi}_e)$, is minimal. The support of a vector $\boldsymbol{\psi}$ is defined as the set of reactions ρ for which $\psi_\rho \neq 0$ and it is minimal if there is no $\boldsymbol{\psi}' \in \ker(\mathbb{S}^X)$ such that $\mathrm{supp}(\boldsymbol{\psi}') \subset \mathrm{supp}(\boldsymbol{\psi})$. As a direct consequence of this minimality, the support of each EFM $\boldsymbol{\psi}_e$ defines a different *unicyclic* subnetwork. EFMs are defined up to a multiplicative constant and can thus be rescaled to have integer entries. They can also be divided into *external* and *internal* EFMs depending on whether their completion has a net effect on the chemostats, $\mathbb{S}^Y \boldsymbol{\psi}_e \neq 0$, or not. In Fig. 1 b), we illustrate the three external EFMs of the CRN. As in this example, their number is generally greater than a fundamental set, a basis for cycles, and tends to grow exponentially with the network size. Despite the development of efficient algorithms [18], the complete enumeration of EFMs remains computationally intensive for large CRNs [8].

Conformal decomposition of the stationary flux - We briefly revisit a known mathematical result [19] which will later gain thermodynamic significance. A vector $\boldsymbol{\varphi}$ is *conformal* to $\boldsymbol{\phi}$ if, for any component ρ, $\varphi_\rho \neq 0 \implies \mathrm{sgn}(\varphi_\rho) = \mathrm{sgn}(\phi_\rho)$. Geometrically, $\boldsymbol{\varphi}$ belongs to the same hyperoctant as $\boldsymbol{\phi}$. Note that, due to zero components, this relation is not always reciprocal: $\boldsymbol{\varphi}$ conf to $\boldsymbol{\phi} \not\Longrightarrow \boldsymbol{\phi}$ conf to $\boldsymbol{\varphi}$. A *conformal decomposition* of $\boldsymbol{\phi}$ is a sum of vectors $\boldsymbol{\varphi}_k$, $\boldsymbol{\phi} = \sum_k \boldsymbol{\varphi}_k$, all conformal to it. One can think of it as a decomposition without cancelation: for any component ρ, all $\varphi_{k\rho}$ have the same sign; see Fig. 1 c). As proved in [19], any steady state current $\boldsymbol{J}^{\mathrm{ss}}$ flowing in the CRN can be decomposed in terms of conformal elementary flux modes (cEFMs), i.e.

$$\boldsymbol{J}^{\mathrm{ss}} = \sum_c j_c \boldsymbol{\psi}_c, \tag{1}$$

where the vectors $j_c \boldsymbol{\psi}_c$ are conformal to $\boldsymbol{J}^{\mathrm{ss}}$ and lin-

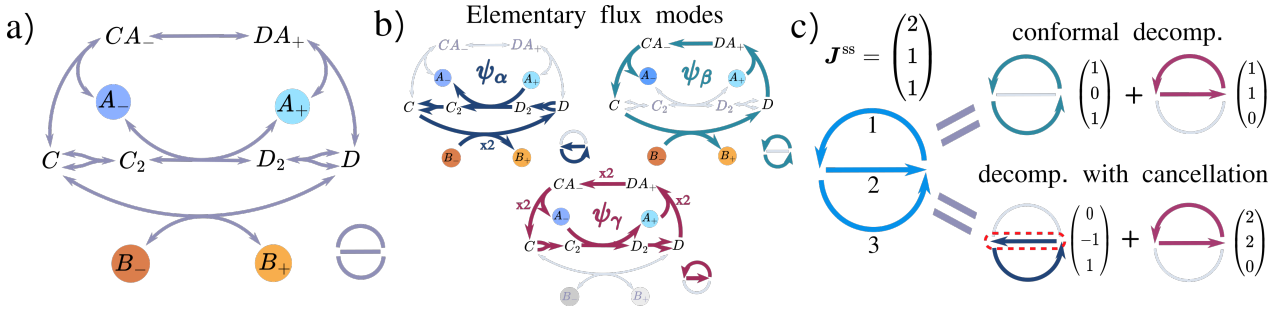

FIG. 1. **a)** Example of a nonlinear multicyclic CRN. The chemostatted species are colored. In the bottom right, a schematic representation of the CRN highlighting its cycle structure. **b)** Elementary flux modes (EFMs) of the CRN $\boldsymbol{\psi}_\alpha, \boldsymbol{\psi}_\beta$, and $\boldsymbol{\psi}_\gamma$ (vectors in the space of reactions) topologically defined as the cycles for the internal species involving a minimal set of reactions. They identify all possible unicyclic subnetworks. **c)** Conformal (top) and non-conformal (bottom) decomposition of the same steady state flux. In the conformal one, the decomposing vectors (EFMs) are aligned with the flux.

early independent. This independence guarantees that any stationary flux can be decomposed with a number of cEFMs $\leq \dim(\ker(\mathbb{S}^X))$. However, we stress that the set of cEFMs used varies with the specific $\boldsymbol{J}^{\rm ss}$ and that this decomposition is not unique. The proof of this result is given in Appendix I. When applied to the example of Fig. 1 a), we find that any stationary current can be decomposed using at most two cEFMs.

cEFM-decomposition of the EP - Using Eq. (1), we can now decompose the stationary EP in terms of cEFMs. At this level, we consider a well-stirred CRN that can be either deterministic or stochastic [20]; in the second case, the following discussion holds for average values. In the derivation, we also assume the *local* validity of the second law, i.e. $\dot{\Sigma}^{\rm ss}_\rho = J^{\rm ss}_\rho \mathcal{A}^{\rm ss}_\rho \geq 0$ and $\mathcal{A}^{\rm ss}_\rho = 0 \iff J^{\rm ss}_\rho = 0$ for any ρ (with finite reaction rates). $\mathcal{A}^{\rm ss}_\rho = -\Delta G^{\rm ss}_\rho$ is the reaction affinity equal to minus the Gibbs free energy change. This implies that $\boldsymbol{J}^{\rm ss}$ and $\boldsymbol{\mathcal{A}}^{\rm ss}$ are reciprocally conformal. We emphasize that this assumption encompasses a large number of cases. In particular, any coarse-graining into a single effective step of multiple reactions that form one emergent cycle (see App. II) preserves the local validity of the second law [21]. Using Eq. (1), the EP can be decomposed as

$$\dot{\Sigma}^{\rm ss} = \boldsymbol{J}^{\rm ss} \cdot \boldsymbol{\mathcal{A}}^{\rm ss} = \sum_c j_c \boldsymbol{\psi}_c \cdot \boldsymbol{\mathcal{A}}^{\rm ss} = \sum_c j_c \mathcal{A}^{\rm ss}_c. \qquad (2)$$

By transitivity, each $j_c\boldsymbol{\psi}_c$, in addition to being conformal to $\boldsymbol{J}^{\rm ss}$, is also conformal to $\boldsymbol{\mathcal{A}}^{\rm ss}$. This implies that the cEFM currents j_c are aligned with the corresponding cycle affinities $\mathcal{A}^{\rm ss}_c$ and that the contribution to the dissipation from each cEFM is positive: $\dot{\Sigma}^{\rm ss}_c = j_c \mathcal{A}^{\rm ss}_c > 0$. Therefore, the cEFMs in Eq. (1) have nonzero affinities and are external, $0 \neq \mathcal{A}^{\rm ss}_c = -\boldsymbol{\mu}\,\mathbb{S}\,\boldsymbol{\psi}_c = -\boldsymbol{\mu}_Y \mathbb{S}^Y \boldsymbol{\psi}_c$. It is interesting to compare this EP decomposition with those previously known in terms of reactions and emergent cycles [22]:

$$\dot{\Sigma}^{\rm ss} = \sum_\rho J^{\rm ss}_\rho \mathcal{A}^{\rm ss}_\rho \quad \text{where} \quad J^{\rm ss}_\rho \mathcal{A}^{\rm ss}_\rho \geq 0, \qquad (3)$$

$$\dot{\Sigma}^{\rm ss} = \sum_\epsilon j^{\rm ss}_\epsilon \mathcal{A}^{\rm ss}_\epsilon \geq 0. \qquad (4)$$

In Eq. (3), all terms are individually nonnegative, but the reaction affinities $\mathcal{A}^{\rm ss}_\rho$ also depend on the chemical potentials $\mu^{\rm ss}_X$ of the internal species. For instance, the affinity of the lowermost reaction in Fig. 1 a) is equal to $\mu^{\rm ss}_C - \mu^{\rm ss}_D + \mu_{B_-} - \mu_{B_+}$. Instead, the emergent cycle affinities $\mathcal{A}^{\rm ss}_\epsilon$ only depend on μ_Y, but the individual terms in Eq. (4) are no longer guaranteed to be nonnegative. Our new decomposition, Eq. (2), combines the advantages of the previous two: $j_c\mathcal{A}^{\rm ss}_c > 0$ for every cEFM and $\mathcal{A}^{\rm ss}_c = -\boldsymbol{\mu}_Y \mathbb{S}^Y \boldsymbol{\psi}_c$ depends only on μ_Y. However, let us note that while in Eq. (4) the set of emergent cycles, once chosen, can be fixed, in Eq. (2) the set of cEFMs varies with the specific $\boldsymbol{J}^{\rm ss}$, which changes, for example, when the chemical potentials μ_Y change. In addition, if the maximum number of cEFMs needed is $N_c = \dim(\ker(\mathbb{S}^X))$, the number of emergent cycles required in Eq. (4) is at most $N_\epsilon = N_c$ - $\dim(\ker(\mathbb{S}))$, see Appendix II. Finally, we note that when the CRN reduced to the X species defines a linear network, Hill found in Ref. [7] an EP decomposition similar to Eq. (2), but where *all* EFMs appear. In that case, the EFMs correspond to the graph cycles, and their coefficients to the net rates at which the EFMs are run under stationary conditions.

Free energy transduction - We now proceed to show why EFMs can be seen as transduction gears of the CRN and how to identify the optimal EFM as a function of the operating conditions. All possible stationary chemical processes among the chemostats Y are given by $\mathrm{Im}(\mathbb{S}^Y\boldsymbol{\psi})$ where $\boldsymbol{\psi} \in \mathrm{Ker}(\mathbb{S}^X)$ is a flux mode. As for EFMs, we identify *elementary processes* as the minimal support vectors of this subspace, equivalent to the conversion modes introduced in [23]. We focus on the canonical transduction scenario, where there are two of them, a and b, which implies $\dim(\mathrm{Im}(\mathbb{S}^Y\boldsymbol{\psi})) = 2$. We define their forward direction so that their corresponding affinities, $\Delta\mu_a$ and $\Delta\mu_b$, are positive. In the example of Fig. 1 a), $a : A_+ \to A_-$ with $\Delta\mu_a = \mu_{A_+} - \mu_{A_-} > 0$

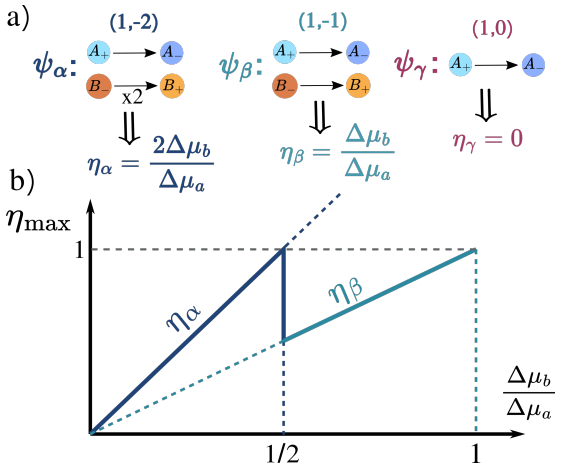

FIG. 2. For the CRN in Fig. 1: **a)** Number of times (m_a, m_b) each EFM consumes processes $a : A_+ \to A_-$ and $b : B_+ \to B_-$ and its associated transduction efficiency; $\boldsymbol{\psi}_\gamma$ is a futile cycle. **b)** Optimal efficiency as a function of the operational conditions $\Delta\mu_b/\Delta\mu_a$. The maximum value is set by the EFM with the highest efficiency < 1, i.e. $\boldsymbol{\psi}_\alpha$ for $\Delta\mu_b < \frac{1}{2}\Delta\mu_a$ and $\boldsymbol{\psi}_\beta$ for $\frac{1}{2}\Delta\mu_a \leq \Delta\mu_b < \Delta\mu_a$.

and $b : B_+ \to B_-$ with $\Delta\mu_b = \mu_{B_+} - \mu_{B_-} > 0$. We note that, in general, a single process can connect more than two chemostats. For example, in the model examined later, in Fig. 3 a), ATP-hydrolysis involves the three chemostatted species ATP, ADP and P_i. EP can be written in terms of these two processes.

$$\dot{\Sigma}^{\rm ss} = \boldsymbol{\mu}_Y \mathbb{S}^Y \boldsymbol{J}^{\rm ss} = J_a^{\rm ss}\Delta\mu_a + J_b^{\rm ss}\Delta\mu_b \geq 0\,. \tag{5}$$

We assume that transduction arises because the spontaneous process a, $J_a^{\rm ss} > 0$, enables the process b to occur against its spontaneous direction, $J_b^{\rm ss} < 0$. The resulting transduction efficiency is thus

$$0 < \eta = \frac{-J_b^{\rm ss}\Delta\mu_b}{J_a^{\rm ss}\Delta\mu_a} < 1. \tag{6}$$

We now assign a transduction efficiency η_e to every external EFM (gear) e. The effect of $\boldsymbol{\psi}_e$ on the chemostats, given by $\mathbb{S}^Y\boldsymbol{\psi}_e$, can be written compactly in terms of two integers (m_a^e, m_b^e) representing respectively the number of times processes a and b are consumed, see Fig. 2 a). For every EFM, we define its forward direction as the one having $m_a^e > 0$ or, in case $m_a^e = 0$, as the one for which $m_b^e > 0$. The EFM's efficiency is then defined as:

$$\eta_e = \frac{-m_b^e\Delta\mu_b}{m_a^e\Delta\mu_a}. \tag{7}$$

Depending on m_a^e, m_b^e, and the ratio $\Delta\mu_b/\Delta\mu_a$, η_e can be negative, if $m_b^e > 0$, bigger than one, or even infinite, if $m_a^e = 0$. For a given $\Delta\mu_b/\Delta\mu_a$, we classify efficiencies as *physical* or *unphysical* according to whether $\eta_e < 1$ or ≥ 1. Given that the EFM cycle affinity is $\mathcal{A}_e^{\rm ss} = m_a^e\Delta\mu_a + m_b^e\Delta\mu_b$, and given that $j_c\mathcal{A}_c^{\rm ss} > 0$ for the cEFMs appearing in the decomposition of Eq. (1), it follows that:

$$\begin{aligned} \eta_c < 1 &\implies \mathcal{A}_c^{\rm ss} > 0 \implies j_c > 0, \\ \eta_c > 1 &\implies \mathcal{A}_c^{\rm ss} < 0 \implies j_c < 0. \end{aligned} \tag{8}$$

In words, whether η_c is physical or not determines the sign of j_c in a conformal decomposition. In particular, only physical cEFMs are run forward. The stationary rates at which the two processes occur are $J_{a/b}^{\rm ss} = \sum_c j_c m_{a/b}^c$ and we can rewrite the overall transduction efficiency η, Eq. (6), as:

$$\eta = \frac{-\sum_c j_c m_b^c \Delta\mu_b}{\sum_c j_c m_a^c \Delta\mu_a} = \frac{\sum_c j_c m_a^c\,\eta_c}{\sum_c j_c m_a^c}. \tag{9}$$

Care must be taken in the last passage when $m_a^c = 0$. This case, together with case $m_b^c = 0$, represents *futile* cEFMs that do not couple the two processes. From the middle expression above, one can see that they always lower the efficiency. Eq. (9) combined with Eq. (8) allows us to upper bound η:

$$\eta \leq \max_{\eta_c<1}\eta_c \leq \max_{\eta_e<1}\eta_e = \eta_{\max}\left(\frac{\Delta\mu_b}{\Delta\mu_a}\right). \tag{10}$$

The proof of this inequality is given in Appendix III. Its interpretation is the following: η is bounded by the optimal EFM, that is, the gear with the highest physical efficiency for the given working conditions. This upper bound can be saturated only by concentrating all the flux on this particular EFM. In Fig. 2 b), we plot Eq. (10) as a function of the operational conditions for the CRN of Fig. 1 a). We note that, in the case of reverse transduction, from b to a, the EFMs efficiencies become $\eta_e^{\rm rev} = \frac{1}{\eta_e}$ and the rest is analogous.

Tight vs. loose coupling - With the result of Eq. (10), we can draw a comparison between the efficiency of a multicyclic CRN and its tightly coupled counterparts, i.e. its EFMs taken individually. At constant operational conditions, $\Delta\mu_b/\Delta\mu_a$ fixed, Eq. (10) tells us that the optimal EFM will always be more efficient than the original loosely coupled CRN. But the latter is more versatile as, in certain conditions, it has the ability to transduce in both directions by properly tuning the reaction rates. This is the case in Fig. 2 b) when $\frac{1}{2} \leq \Delta\mu_b/\Delta\mu_a < 1$ and $\eta_\alpha^{\rm rev}, \eta_\beta < 1$. When considering variable working conditions, $\Delta\mu_b/\Delta\mu_a$ can change in a given range, say $\Delta\mu_b/\Delta\mu_a \in \left[\frac{1}{4}, \frac{3}{4}\right]$ in Fig. 2 b), optimality becomes context dependent. A given EFM may only transduce in a fraction of the operating range, as α in Fig. 2 b), or be less efficient than the loosely coupled CRN in certain regions of the operating range, as β. Combining optimality and versatility requires a loosely coupled CRN that can autonomously switch EMF (gear) depending on the working conditions.

Self-regulating CRN - We now propose a simple model explaining how such gear shifting may autonomously take

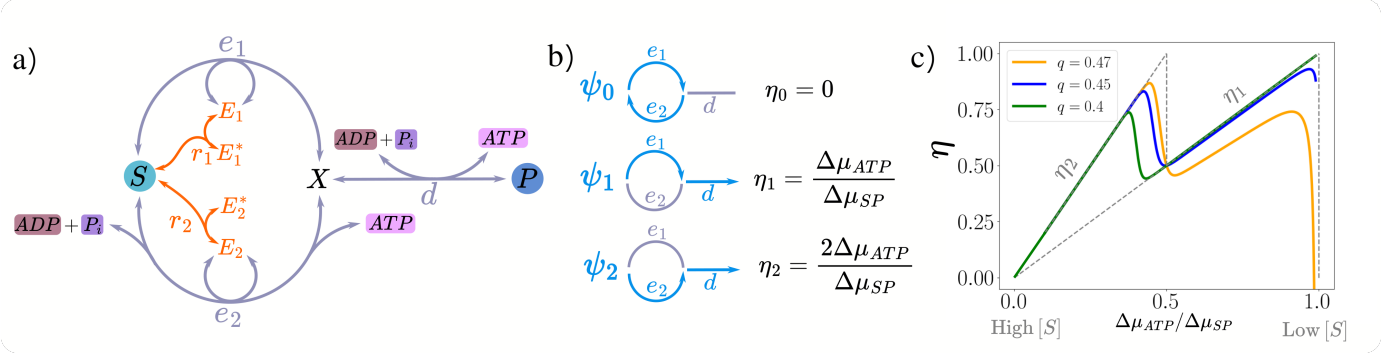

FIG. 3. **a)** Self-regulating CRN; see model in Eq. (11). The chemostatted species are colored. The substrate S, through the enzymes E_1 and E_2, controls the flow of the reactions e_1 and e_2 favoring the latter. **b)** The three EFMs $\boldsymbol{\psi}_0, \boldsymbol{\psi}_1$, and $\boldsymbol{\psi}_2$ of the CRN (schematic representation) with their corresponding transduction efficiencies; $\boldsymbol{\psi}_0$ is a futile cycle. **c)** Efficiency of the CRN as a function of the operational condition $\Delta\mu_{ATP}/\Delta\mu_{SP}$ ($\Delta\mu_{ATP} = 20k_bT$). q is the effective value on the x axis at which the CRN switches gear, passing from $\boldsymbol{\psi}_2$ to $\boldsymbol{\psi}_1$. The uppermost dotted line represents the maximum achievable value for η given by Eq. (10).

place in biochemistry. We consider the CRN in Fig. 3 a) with chemostatted species $Y = S, P, ADP, P_i, ATP$. This CRN couples the conversion $S \to P$, $\Delta\mu_{SP} > 0$, to the synthesis $ADP + P_i \to ATP$, $\Delta\mu_{ATP} > 0$. Two transducing EFMs are present: $\boldsymbol{\psi_1}$ and $\boldsymbol{\psi_2}$, see Fig. 3 b), with efficiencies $\eta_1 = \Delta\mu_{ATP}/\Delta\mu_{SP} = \eta_2/2$. The flow through the network is regulated by the enzymes E_1 and E_2 that act on the reactions e_1 and e_2. Their concentrations are in turn controlled by S through reactions r_1 and r_2. The resulting effect is that the presence of S favors $\boldsymbol{\psi_2}$ over $\boldsymbol{\psi_1}$ because S inhibits E_1 by transforming it into E_1^* and activates E_2^* by converting it to E_2. This is the desired switch to maximize efficiency: the higher the concentration of S, the higher the chemical potential $\Delta\mu_{SP}$, and thus the more convenient it becomes to operate with a "heavier" gear like $\boldsymbol{\psi_2}$. We assign the reaction rates according to the mass-action law:

$$
\begin{aligned}
r_1 &: E_1 + S \underset{k_r[E_1^*][\bar{S}]}{\overset{k_r[E_1][S]}{\rightleftharpoons}} E_1^* \qquad r_2 : E_2^* + S \underset{k_r[E_2][\bar{S}]}{\overset{k_r[E_2^*][S]}{\rightleftharpoons}} E_2, \\
e_1 &: E_1 + S \underset{k_e[E_1][X]}{\overset{k_e[E_1][S]}{\rightleftharpoons}} X + E_1, \\
e_2 &: E_2 + ADP + P_i + S \underset{k_e \exp(\Delta\mu_{ATP})[E_2][X]}{\overset{k_e[E_2][S]}{\rightleftharpoons}} X + ATP + E_2, \\
d &: ADP + P_i + X \underset{k_d \exp(\Delta\mu_{ATP})[P]}{\overset{k_d \exp(\Delta\mu_{SP}^0)[X]}{\rightleftharpoons}} P + ATP. \qquad (11)
\end{aligned}
$$

$[\alpha]$ and μ_α denote the concentration and chemical potential of species α. For ideal-dilute solutions, it is $\mu_\alpha = \mu_\alpha^0 + \log([\alpha])$ measured in units of RT. In addition, $\Delta\mu_{SP}^0 = \Delta\mu_S^0 - \Delta\mu_P^0$ and we assume $\mu_S^0 = \mu_X^0$. $[\bar{S}]$ is a parameter with the dimension of a concentration defining the backward rates in the first two reactions. The above rates are thermodynamically consistent since they satisfy the local detailed balance condition [24]. We set the total concentrations of the two enzymes equal to the same value $L = [E_i^*] + [E_i]$. From the rates in Eq. (11), it follows $[E_1]/[E_2] = [\bar{S}]/[S]$ at steady state. We assume $k_d \gg k_e L$ so that reaction d is effectively at equilibrium and thus $[X] \approx e^{\Delta\mu_{ATP} - \Delta\mu_{SP}^0}[P]$. From the knowledge of $[X]$ and the rates in Eq. (11), one can easily derive the reaction currents J_{e_1} and J_{e_2}. The transduction efficiency is then given by:

$$
\eta = \frac{J_{e_1} + 2J_{e_2}}{J_{e_1} + J_{e_2}} \frac{\Delta\mu_{ATP}}{\Delta\mu_{SP}} = g \frac{\Delta\mu_{ATP}}{\Delta\mu_{SP}}, \qquad (12)
$$

where

$$
g = \frac{e^{\Delta\bar{\mu}_{SP}}(e^{\Delta\mu_{SP}} - e^{\Delta\mu_{ATP}}) + 2e^{\Delta\mu_{SP}}(e^{\Delta\mu_{SP}} - e^{2\Delta\mu_{ATP}})}{e^{\Delta\bar{\mu}_{SP}}(e^{\Delta\mu_{SP}} - e^{\Delta\mu_{ATP}}) + e^{\Delta\mu_{SP}}(e^{\Delta\mu_{SP}} - e^{2\Delta\mu_{ATP}})},
$$

and $\Delta\bar{\mu}_{SP} = \mu_S^0 + \log[\bar{S}] - \mu_P$. In Fig. 3 c), we report this efficiency η as a function of $\Delta\mu_{ATP}/\Delta\mu_{SP}$ that varies due to changes in S while keeping everything else fixed. The parameter $q = \Delta\mu_{ATP}/\Delta\bar{\mu}_{SP}$ represents the effective position on the x axis at which gear switching occurs: at that value, $[S] = [\bar{S}]$ and $[E_1] = [E_2]$. To preserve transduction, one needs $q < \frac{1}{2}$, that is, $\boldsymbol{\psi}_2$ has to be down-regulated before its affinity changes sign. The smaller q, the less efficient the CRN will be before $\Delta\mu_{ATP}/\Delta\mu_{SP} = \frac{1}{2}$, and the more efficient it will be above that value. We only considered substrate inhibition of the enzymes in our model, but extensions to other types of regulation (by product P or ADP, ATP) are possible.

Conclusion - Our work provides a rigorous framework for analyzing energy transduction in metabolic CRNs, in particular their efficiency and regulation. Our precise notion of transduction gears may help improve our understanding of metabolic switches and the extent to which they are driven by the need to maintain high thermodynamic efficiencies.

Acknowledgements MB is funded by AFR PhD grant 15749869 funded by Luxembourg National Research Fund (FNR) and ME by CORE project ChemComplex (Grant No. C21/MS/16356329), and by project INTER/FNRS/20/15074473 funded by F.R.S.-FNRS

(Belgium) and FNR.

Appendix I: Conformal decomposition of the stationary flux

The proof is readapted from [19] and proceeds by induction on the cardinality of $\mathrm{supp}(\boldsymbol{J}^{\mathrm{ss}})$ and makes use of the following lemma.

Lemma. Given $\boldsymbol{\psi} \in \ker(\mathbb{S}^X)$, one can always find a EFM conformal to it.

Proof If $\boldsymbol{\psi}$ is an EFM, the lemma is trivially true. Otherwise, we show that one can build a vector $\boldsymbol{\psi}'' \in \ker(\mathbb{S}^X)$ conformal to $\boldsymbol{\psi}$ that has a smaller support. When $\boldsymbol{\psi}$ is not an EFM, it is, by definition, not support minimal. Thus, there exists $\boldsymbol{\psi}' \in \ker(\mathbb{S}^X)$ such that $\mathrm{supp}(\boldsymbol{\psi}') \subset \mathrm{supp}(\boldsymbol{\psi})$. If $\pm\boldsymbol{\psi}'$ is conformal to $\boldsymbol{\psi}$, then $\boldsymbol{\psi}'' = \pm\boldsymbol{\psi}'$. If not, $\boldsymbol{\psi}'' = \boldsymbol{\psi} - \lambda\boldsymbol{\psi}'$ where $\lambda > 0$ is the highest value for which $\boldsymbol{\psi}''$ is still conformal to $\boldsymbol{\psi}$. By subtracting $\lambda\boldsymbol{\psi}'$, we cancel a component of $\boldsymbol{\psi}$ resulting in $\mathrm{supp}(\boldsymbol{\psi}'') \subset \mathrm{supp}(\boldsymbol{\psi})$. Now, if $\boldsymbol{\psi}''$ is a cEFM, the lemma is satisfied; otherwise, we can repeat the above procedure until the final vector is support minimal and thus a cEFM.

Since $\boldsymbol{J}^{\mathrm{ss}} \in \ker(\mathbb{S}^X)$, the lemma ensures the existence of a conformal EFM $\boldsymbol{\psi}_c$. Through $\boldsymbol{\psi}_c$, we can build a vector $\boldsymbol{J}^*$ conformal to $\boldsymbol{J}^{\mathrm{ss}}$ such that $\mathrm{supp}(\boldsymbol{J}^*) \subset \mathrm{supp}(\boldsymbol{J}^{\mathrm{ss}})$. It suffices to choose, in the expression $\boldsymbol{J}^* = \boldsymbol{J}^{\mathrm{ss}} - j_c^*\boldsymbol{\psi}_c$, the maximum $j_c^* > 0$ for which $\boldsymbol{J}^*$ is still conformal to $\boldsymbol{J}^{\mathrm{ss}}$. Then, the induction hypothesis tells us that $\boldsymbol{J}^*$ admits a conformal decomposition in terms of linearly independent cEFMs: $\boldsymbol{J}^* = \sum_{c'} j_{c'}\boldsymbol{\psi}_{c'}$. Since $\mathrm{supp}(\boldsymbol{\psi}_c) \not\subset \mathrm{supp}(\boldsymbol{J}^*)$, $\boldsymbol{\psi}_c$ is also independent of all the other $\boldsymbol{\psi}_{c'}$. Therefore, the desired conformal decomposition for $\boldsymbol{J}^{\mathrm{ss}}$ follows:

$$\boldsymbol{J}^{\mathrm{ss}} = j_c^*\boldsymbol{\psi}_c + \boldsymbol{J}^* = j_c^*\boldsymbol{\psi}_c + \sum_{c'} j_{c'}\boldsymbol{\psi}_{c'}. \tag{13}$$

Appendix II: Relation between internal / emergent cycles and EFM

Internal cycles are defined as a set of independent vectors $\{\boldsymbol{c}_i\}$ that span $\ker(\mathbb{S})$: their completion has no net effect on the concentration of the X and Y species. Emergent cycles are then a set of vectors $\{\boldsymbol{c}_\epsilon\}$ that, together with the $\{\boldsymbol{c}_i\}$, form a basis for $\ker(\mathbb{S}^X)$ [22]: contrary to internal cycles, they alter the chemostats $\mathbb{S}^Y\boldsymbol{c}_\epsilon \neq 0$. Their respective numbers are $N_i = \dim(\ker(\mathbb{S}))$ and $N_\epsilon = \dim(\ker(\mathbb{S}^X)) - \dim(\ker(\mathbb{S}))$ and the choice of these sets is arbitrary. Internal EFMs are vectors lying in $\ker(\mathbb{S})$ and therefore linear combinations of $\{\boldsymbol{c}_i\}$. The maximum number of independent internal EFMs is N_i and they can be chosen as the set of internal cycles, as done in [25]. External EFMs are located in $\ker(\mathbb{S}^X)$ and are generally linear combinations of both internal and emergent cycles. The number of independent external EFMs is $\leq N_i + N_\epsilon = \dim(\ker(\mathbb{S}^X))$. Also in this case, a subset of them can be chosen to form the set of emergent cycles. From this perspective, the EP decomposition of Eq. (2) represents a special case of the decomposition of Eq. (4).

Appendix III: Upper bound on transduction efficiency

We prove Eq. (10) starting from the expression in Eq. (9). We divide the set of cEFMs into physical and unphysical: $\{c\} = \{c'\} + \{c''\}$ with $\eta_{c'} < 1$ and $\eta_{c''} \geq 1$. From Eq. (8), we have $j_{c'} > 0$ and $j_{c''} < 0$, which implies that the coefficients $r_{c'} = j_{c'}m_a^{c'}$ and $q_{c''} = -j_{c''}m_a^{c''}$ are both nonnegative since $m_a^f \geq 0$. We can therefore express the efficiency in Eq. (9) in terms of them as:

$$\eta = \frac{\sum_{c'} r_{c'}\eta_{c'} - \sum_{c''} q_{c''}\eta_{c''}}{\sum_{c'} r_{c'} - \sum_{c''} q_{c''}}. \tag{14}$$

We first show that every $q_{c''} \neq 0$ negatively affects the efficiency compared to the case where the same $q_{c''}$ is zero. To do this, we rewrite the efficiency as follows.

$$\eta = \frac{C - q_{c''}\eta_{c''}}{D - q_{c''}}, \tag{15}$$

where all the other terms have been reabsorbed into the constants C and D. Both the numerator and the denominator are positive since the CRN is performing transduction. In addition, $C < D\,\eta_{c''}$ must hold to have $\eta < 1$, which is enough to prove that $\eta < C/D$. Repeating this argument for all the cEFMs in $\{c''\}$, one obtains:

$$\eta \leq \frac{\sum_{c'} r_{c'}\eta_{c'}}{\sum_{c'} r_{c'}}. \tag{16}$$

The RHS is simply a weighted average with positive coefficients and therefore Eq. (10) follows.

* massimo.bilancioni@uni.lu
† massimiliano.esposito@uni.lu

[1] M. Cox and D. Nelson, *Lehninger Principles of Biochemistry*, Vol. 5 (2000).
[2] D. Voet, J. Voet, and C. Pratt, *Fundamentals of Biochemistry: Life at the Molecular Level* (Wiley, 2016).
[3] X. Yang, M. Heinemann, J. Howard, G. Huber, S. Iyer-Biswas, G. L. Treut, M. Lynch, K. L. Montooth, D. J. Needleman, S. Pigolotti, J. Rodenfels, P. Ronceray, S. Shankar, I. Tavassoly, S. Thutupalli, D. V. Titov, J. Wang, and P. J. Foster, Physical bioenergetics: Energy fluxes, budgets, and constraints in cells, Proceedings

of the National Academy of Sciences **118**, e2026786118 (2021).
[4] A. I. Brown and D. A. Sivak, Theory of nonequilibrium free energy transduction by molecular machines, Chemical Reviews **120**, 10.1021/acs.chemrev.9b00254 (2020).
[5] A. Wachtel, R. Rao, and M. Esposito, Free-energy transduction in chemical reaction networks: From enzymes to metabolism, The Journal of Chemical Physics **157**, 024109 (2022).
[6] A. Parmeggiani, F. Jülicher, A. Ajdari, and J. Prost, Energy transduction of isothermal ratchets: Generic aspects and specific examples close to and far from equilibrium, Phys. Rev. E **60**, 2127 (1999).
[7] T. L. Hill, Chapter 3 - fluxes and forces, in *Free Energy Transduction in Biology*, edited by T. L. Hill (Academic Press, 1977).
[8] J. Zanghellini, D. E. Ruckerbauer, M. Hanscho, and C. Jungreuthmayer, Elementary flux modes in a nutshell: Properties, calculation and applications, Biotechnology Journal **8**, 1009 (2013).
[9] M. Yasemi and M. Jolicoeur, Modelling cell metabolism: A review on constraint-based steady-state and kinetic approaches, Processes **9**, 10.3390/pr9020322 (2021).
[10] C. T. Trinh, A. Wlaschin, and F. Srienc, Elementary mode analysis: a useful metabolic pathway analysis tool for characterizing cellular metabolism, Applied Microbiology and Biotechnology **81**, 813 (2009).
[11] F. Rojo, Carbon catabolite repression in Pseudomonas: optimizing metabolic versatility and interactions with the environment, FEMS Microbiology Reviews **34**, 658 (2010).
[12] R. H. De Deken, The crabtree effect: A regulatory system in yeast, Microbiology **44**, 149 (1966).
[13] O. Frick and C. Wittmann, Characterization of the metabolic shift between oxidative and fermentative growth in saccharomyces cerevisiae by comparative 13c flux analysis, Microbial Cell Factories **4**, 30 (2005).
[14] A. I. Mahmoud, Metabolic switches during development and regeneration, Development **150**, dev202008 (2023).
[15] T. Koyama, M. J. Texada, K. A. Halberg, and K. Rewitz, Metabolism and growth adaptation to environmental conditions in drosophila, Cellular and Molecular Life Sciences **77**, 4523 (2020).
[16] R. Karimi, A. Cleven, F. Elbarbry, and H. Hoang, The impact of fasting on major metabolic pathways of macronutrients and pharmacokinetics steps of drugs, European Journal of Drug Metabolism and Pharmacokinetics **46**, 25 (2021).
[17] Y. Zhang and H. V. Westerhoff, Gear shifting in biological energy transduction, Entropy **25**, 10.3390/e25070993 (2023).
[18] M. Terzer and J. Stelling, Large-scale computation of elementary flux modes with bit pattern trees, Bioinformatics **24**, 2229 (2008).
[19] S. Müller and G. Regensburger, Elementary vectors and conformal sums in polyhedral geometry and their relevance for metabolic pathway analysis, Frontiers in Genetics **7**, 10.3389/fgene.2016.00090 (2016).
[20] R. Rao and M. Esposito, Conservation laws and work fluctuation relations in chemical reaction networks, The Journal of Chemical Physics **149**, 245101 (2018).
[21] F. Avanzini, N. Freitas, and M. Esposito, Circuit theory for chemical reaction networks, Phys. Rev. X **13**, 021041 (2023).
[22] M. Polettini and M. Esposito, Irreversible thermodynamics of open chemical networks. I. Emergent cycles and broken conservation laws, The Journal of Chemical Physics **141**, 024117 (2014).
[23] R. Urbanczik and C. Wagner, Functional stoichiometric analysis of metabolic networks, Bioinformatics **21**, 4176 (2005).
[24] R. Rao and M. Esposito, Nonequilibrium thermodynamics of chemical reaction networks: Wisdom from stochastic thermodynamics, Phys. Rev. X **6**, 041064 (2016).
[25] S. Dal Cengio, V. Lecomte, and M. Polettini, Geometry of nonequilibrium reaction networks, Phys. Rev. X **13**, 021040 (2023).